Color performance of an MVA-LCD using an LED backlight

Ruibo Lu (SID Member)
Xiangyi Nie
Shin-Tson Wu (SID Fellow)

Abstract — The color performance, including color gamut, color shift, and gamma curve, of a multi-domain vertical-alignment (MVA) liquid-crystal display (LCD) using an LED backlight are calculated quantitatively. Simulation results indicate that an LED backlight exhibits better angular color uniformity and smaller color shifts than a CCFL backlight. Color gamut can be further widened and color shift reduced when using a color-sequential RGB-LED backlight without color filters, while the angular-dependent gamma curves are less influenced using different backlights. The obtained quantitative results are useful for optimizing the color performance and color management of high-end LCD monitors and LCD TVs.

Keywords — *Liquid-crystal display, multi-domain vertical alignment, color, LED backlight.*
DOI # 10.1889/JSID16.11.1139

1 Introduction

Liquid-crystal displays (LCDs) using a light-emitting-diode (LED) backlight unit show evident performance advantages over the conventional cold-cathode fluorescent lamp (CCFL) such as wider color gamut; higher brightness; tunable backlight white-point control by separate red, green, and blue (RGB) colors; real-time color management, *etc.*[1–3] For high-end LCD monitors and TVs, weak color shift, fast response time, wide viewing angle, high contrast ratio, and high optical efficiency are critically important. To meet these technical challenges, the multi-domain vertical-alignment (MVA) LCDs have been developed and widely used.[4,5]

In this paper, the color performance of a film-compensated MVA-LCD using an LED backlight is quantitatively evaluated in terms of color gamut, color shift, and gamma curves. These results are compared with an MVA-LCD using a conventional CCFL backlight. We calculated the color shift based on the color difference in CIE-1976 uniform chromaticity scale. The optical properties of the LCDs are simulated using a 3-D simulator, and these results are imported for calculating the color performances.

2 Modeling of color shift

The CIE XYZ color space defines all the colors in terms of three imaginary primaries X, Y, and Z based on the human visual system. The X, Y, Z tristimulus values of a color stimulus [$S(\lambda)$], which represent the luminance or lightness of the colors are expressed as

$$X = k\int_{380\,\mathrm{nm}}^{780\,\mathrm{nm}} S(\lambda)\bar{x}(\lambda)\,d\lambda,\quad Y = k\int_{380\,\mathrm{nm}}^{780\,\mathrm{nm}} S(\lambda)\bar{y}(\lambda)\,d\lambda,\quad Z = k\int_{380\,\mathrm{nm}}^{780\,\mathrm{nm}} S(\lambda)\bar{z}(\lambda)\,d\lambda. \tag{1}$$

Here, the values of $\bar{x}(\lambda)$, $\bar{y}(\lambda)$, and $\bar{z}(\lambda)$ color-matching functions are the tristimulus values of the monochromatic stimuli, $S(\lambda)$ represents the spectral radiometric quantity at wavelength λ, *e.g.*, it is the light-transmission intensity in a practical LCD device in consideration of the used backlight source and the color filters, and k is a constant.[6,7]

The CIE-1976 uniform chromaticity scale (UCS) diagram, which is also called the (u', v') diagram, has been commonly used to present the equidistant chromaticity scales. The (u', v') coordinates are related to the (x, y) coordinates in CIE 1931 by the following equations:

$$u' = \frac{4X}{X+15Y+3Z} = \frac{4X}{-2x+12y+3},\qquad v' = \frac{9Y}{X+15Y+3Z} = \frac{9y}{-2x+12y+3} \tag{2}$$

Based on Eq. (2), $\Delta u'v'$ at any two positions (1 and 2) can be calculated using the following formula:

$$\Delta u'v' = \sqrt{(u'_2-u'_1)^2+(v'_2-v'_1)^2}. \tag{3}$$

To characterize the color shift of an LCD TV, $[u'_2, v'_2]$ represent the $[u', v']$ values at an oblique viewing angle, while $[u'_1, v'_1]$ are usually referred to the $[u', v']$ values at normal viewing angle.

Revised version of a paper presented at the 15th Color Imaging Conference (CIC '07) held November 5–9, 2007 in Albuquerque, New Mexico.
The authors are with the College of Optics and Photonics, University of Central Florida, 4000 Central Florida Blvd., Orlando, FL 32816-2700; telephone 407/823-6822, fax –6800, e-mail: rlu@mail.ucf.edu.

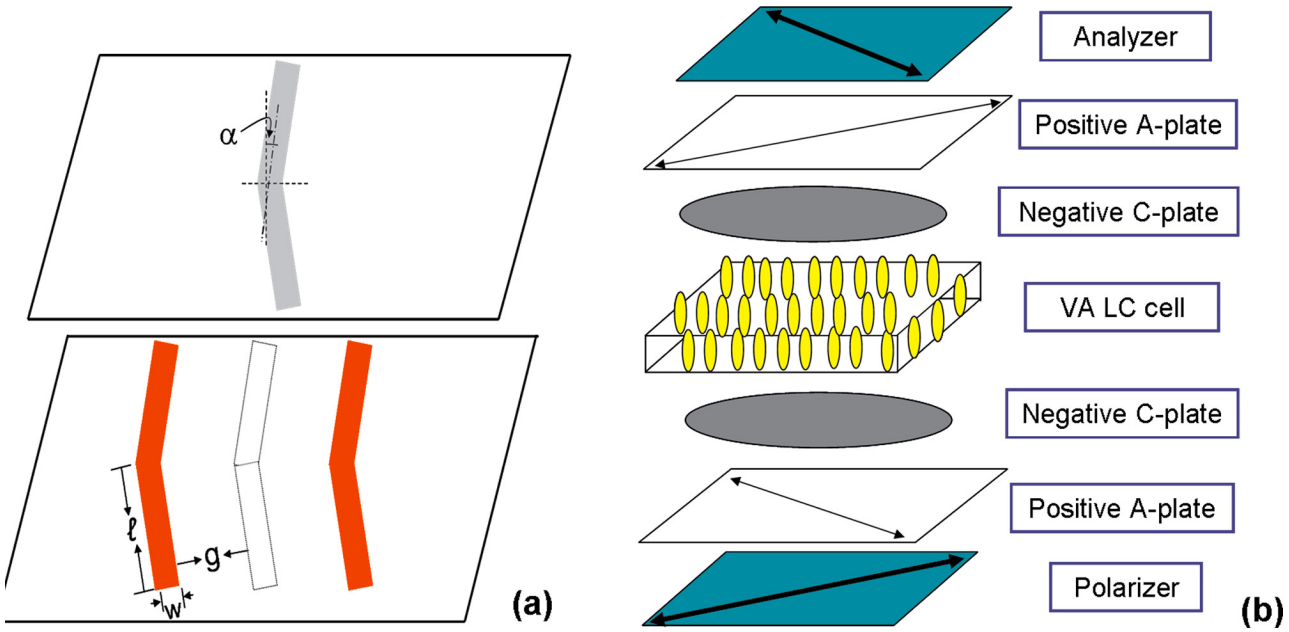

FIGURE 1 — (a) The typical electrode structure and (b) device configuration of the multi-domain LCD.

3 Device structures and simulation methods

Figure 1 shows a typical electrode structure and device configuration of the MVA-LCD, which leads to four domains in the voltage-on state.[8] In our design, we assume the repeated unit pixel size of the MVA-LCD is 100 μm (width) × 300 μm (height). The cell gap of the MVA LCD is d = 4 μm, the width of the chevron-shaped slit is w = 12 μm, the gap between the neighboring slits on the bottom and top substrates is g = 35 μm on the projected plane, and the chevron arm length ℓ = 140 μm. The bending angle is α = 45°, and LC pretilt angle is 90° with respect to the substrate surface. We simulate the MVA-LCD using a Merck negative LC mixture MLC-6608 whose parameters are listed as follows: γ_1 = 0.186 Pa-sec, $\Delta\varepsilon$ = –4.2, K_{11} = 16.7 pN, K_{22} = 7.0 pN, K_{33} = 18.1 pN, and Δn = 0.083 at λ = 550 nm. The birefringence dispersion of the LC material at each wavelength of the light source is included in the calculation using the following equation:[9,10]

$$\Delta n = G \cdot \frac{\lambda^2 \cdot \lambda^{*2}}{\lambda^2 - \lambda^{*2}} \tag{4}$$

At room temperature, the two fitting parameters are $G = 1.608 \times 10^{-6}$ nm^{-2} and λ^* = 210 nm.

In the wide-view MVA-LCD, phase compensation films are required.[11] Here, two sets of uniaxial films, a positive A-plate with $d\cdot\Delta n$ = 93.2 nm and a negative C-plate with $d\cdot\Delta n$ = –85.7 nm are placed after the polarizer and before the analyzer, respectively. The positive A-plate has n_e = 1.5124 and n_o = 1.5089 at λ = 550 nm, and the negative C-plate has n_e = 1.5089 and n_o = 1.5124 at λ = 550 nm.[12] During simulations, we assume the phase-matched compensation films have the same color dispersion as that of the LC material employed.[13] The simulation sequence is to obtain the dynamic 3-D LC director distributions first and then calculate the detailed electro-optics of the LCD. We used a 3-D simulator to calculate the LC director distributions. Once the LC director distribution profiles are obtained, we then calculate the electro-optic properties of the LCD using the extended Jones matrix method.[14,15] The LC layer is modeled as a stack of uniaxial homogeneous layers. Here, we assume the reflections between the interfaces are negligible. Therefore, the transmitted electric field is related to the incident electric field by

$$\begin{bmatrix} E_x \\ E_y \end{bmatrix}_{N+1} = \mathbf{J}\begin{bmatrix} E_x \\ E_y \end{bmatrix}_1 = \mathbf{J}_{Ext}\mathbf{J}_N\mathbf{J}_{N-1}\Lambda\mathbf{J}_2\mathbf{J}_1\mathbf{J}_{Ent}\begin{bmatrix} E_x \\ E_y \end{bmatrix}_1, \tag{5}$$

where $\mathbf{J}_{Ext}$ and $\mathbf{J}_{Ent}$ are the correction matrices considering the transmission losses in the air–LCD interface, which are given by

$$\mathbf{J}_{Ent} = \begin{bmatrix} \dfrac{2\cos\theta_p}{\cos\theta_p + n_p\cos\theta_k} & 0 \\ 0 & \dfrac{2\cos\theta_k}{\cos\theta_k + n_p\cos\theta_p} \end{bmatrix},$$
$$\mathbf{J}_{Ext} = \begin{bmatrix} \dfrac{2n_p\cos\theta_k}{\cos\theta_p + n_p\cos\theta_k} & 0 \\ 0 & \dfrac{2n_p\cos\theta_p}{\cos\theta_k + n_p\cos\theta_p} \end{bmatrix}, \tag{6}$$

Correspondingly, the overall optical transmittance is represented as

$$t_{\mathrm{op}} = \frac{\left|E_{x,N+1}\right| + \cos^2\theta_p \cdot \left|E_{y,N+1}\right|^2}{\left|E_{x,1}\right|^2 + \cos^2\theta_p \cdot \left|E_{y,1}\right|^2}, \quad (7)$$

where τ_p is given by

$$\theta_p = \sin^{-1}\left[\sin\theta_k / \mathrm{Re}(n_p)\right]. \quad (8)$$

Here, $\mathrm{Re}(n_p)$ is the average of the real parts of the two refractive indices ($n_{e,p}$ and $n_{o,p}$) of the polarizer, where $n_{e,p} = 1.500 + I \times 3.251 \times 10^{-3}$ and $n_{o,p} = 1.500 + I \times 2.86 \times 10^{-5}$, and θ_k is the azimuthal angle of the incident wave vector **k**.

4 Results and discussion

4.1 Color gamut of LCD panels with LED and CCFL backlights

Figure 2 shows the transmission spectra of the CCFL and LED backlight units and color filters. The white-LED BLU consists of a series of separate RGB LEDs as shown in Fig. 2(a), and the color filters have their average peak transmittance at R ~ 650 nm, G ~ 550 nm, and B ~ 450 nm [Fig. 2(b)]. The separate RGB LEDs without color filters are usually used in the color-sequential LCDs. It can be seen that the RGB peak wavelengths of the LED BLU match better to those of color filters (CFs), and its respective bandwidth is narrower and without side lobes as compared to that of a CCFL BLU.

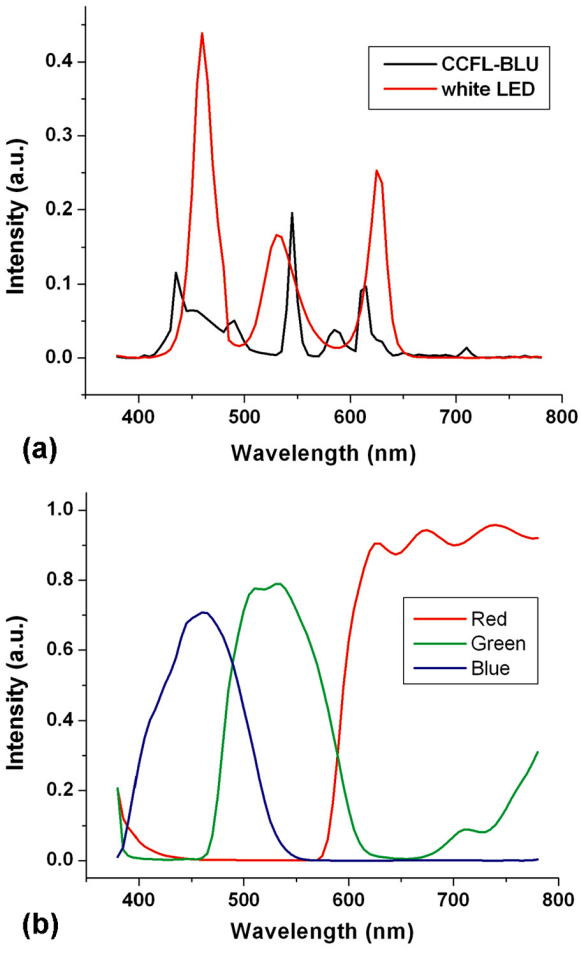

FIGURE 2 — (a) The emission spectra of the CCFL and white-LED BLU and (b) the transmission spectra of CFs.

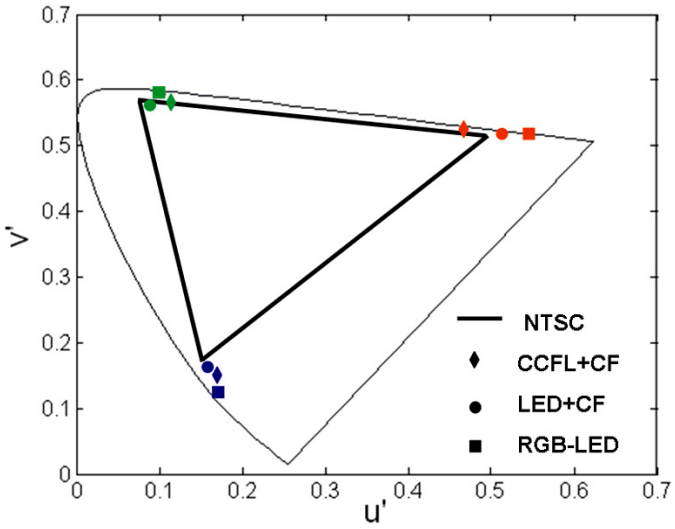

FIGURE 3 — The RGB primaries through the MVA-LCD panel for different backlights and NTSC standard primaries on the CIE 1976 UCS diagram.

Figure 3 is a plot of the RGB primaries through the MVA-LCD panel using a CCFL BLU, a white LED BLU with color filters, or a separate RGB LED without color filters. The color gamut is defined by the color points of the RGB primaries through the LCD panel. From Fig. 3, the color gamut of the white LED BLU with color filters is larger than that of the CCFL primaries and is 114.2% of the National Television System Committee (NTSC) standard primaries. It means that it is possible for an LCD to obtain a color gamut greater than 100% NTSC by properly selecting the LED colors and color filters. As for the primaries of the separate RGB LED without color filters, the color space can be further widened from 114.2% to 128.7% NTSC color gamut. The color gamut of an LCD device using a conventional CCFL BLU is usually about 75% NTSC.[16] Although a wide-gamut CCFL BLU has been commonly adopted by the LCD industry, the color gamut achieved by the CCFL backlight is 95.4% of the NTSC standard, which is still narrower than that of LED backlights. This is because the peak transmittance of the RGB primary colors of the LED BLU match better with those of color filters and their respective bandwidth is narrower as plotted in Fig. 2. Although a wider color gamut is desirable, good color saturation and natural color are equally important.

4.2 Color shift of RGB primaries at different incident angles

LC is a birefringent material; thus, the phase retardation at different gray levels would depend on the light-incident

direction, especially at large oblique angles. This phase difference lead to the angular-dependent color shifts at different gray levels and different backlight sources. The angular-dependent phase retardation of the LC medium at a given wavelength λ can be expressed as[17]:

$$\delta(\theta,\varphi,\alpha,V,\lambda) = 2\pi(d\cdot\Delta n)_{eff}/\lambda, \quad (9)$$

where

$$(d\cdot\Delta n)_{eff} = \frac{d}{\cos\theta}\left\{\frac{n_e n_o}{\sqrt{n_o^2\sin^2(\theta+\alpha)+n_e^2\cos^2(\theta+\alpha)}} - n_o\right\}, \quad (10)$$

In Eqs. (9) and (10), n_o and n_e represent the ordinary and extraordinary refractive indices of LC material, $\Delta n = n_e - n_o$ is the LC birefringence, is the cell gap, θ is the incident angle defined as the angle between the light-incident direction and the normal of the LCD panel, φ is the azimuthal angle of the LCs which is defined as the angle between the effective optic axis of the LC directors and the transmission axis of the polarizer, and α is the LC tilt angle. Correspondingly, the normalized light transmittance (T) through the LC medium under crossed linear polarizers has the following form[18]:

$$T = \sin^2(2\varphi)\sin^2(\delta/2) = \sin^2(2\varphi)\sin^2\left[\pi\cdot(d\cdot\Delta n)_{eff}/\lambda\right]. \quad (11)$$

From Eq. (11), the normalized transmittance, T, is closely related to the light-incident angle, LC orientation angle, incident wavelength of the backlight, and applied voltage corresponding to the different gray levels. As formulated in Eq. (1), $S(\lambda)$ can be represented by the light-transmission intensity in a practical LCD device, which is characterized by the normalized light transmittance, T, in connection with the corresponding transmission spectra of the backlight source and the color filters. Therefore, the (u', v') coordinates are also closely related to these factors.

Figure 4 is the typical plot of the CIE-1976 UCS diagrams with different incident angles at the gray level, G63, for CCFL, white-LED, and RGB-LED backlights. In our calculations, we vary θ from –80° to +80° and scan the backlights across the entire 360° azimuthal angle (ϕ) at a 10° scanning step for every chosen θ. It is evident that the LED-lit LCDs as shown in Figs. 4(b) and 4(c) have a weaker color shift than a CCFL [Fig. 4(a)] in all the RGB primaries, especially when the RGB-LED backlight is used. A similar trend is found at higher gray levels, such as the full bright state, G255.

The above phenomena can be explained as follows. As seen in Fig. 2, the emission spectra of the CCFL-BLU are much wider than that of a white-LED BLU in the visible spectral range. In addition, the RGB peak wavelengths of an LED BLU match better to those of CFs. After the light passes through the CFs, the transmission spectra of a CCFL with CFs are still wider than those of a white LED with CFs in RGB primaries. Correspondingly, the CCFL back-lit MVA-LCD with CFs has a larger spectral range of wavelength-dependent light transmittance, T, to integrate in Eq. (1). This results in larger u' and v' coordinate values in the CIE 1976 UCS diagrams, and therefore the MVA-LCD shows a larger color shift in the respective RGB primaries. In the while the RGB-LED BLU without CFs has the narrowest transmission spectra. This makes the RGB-LED back-lit MVA-LCD without CFs having smaller u' and v' coordinate values in the respective RGB primaries, leading to a weaker color shift.

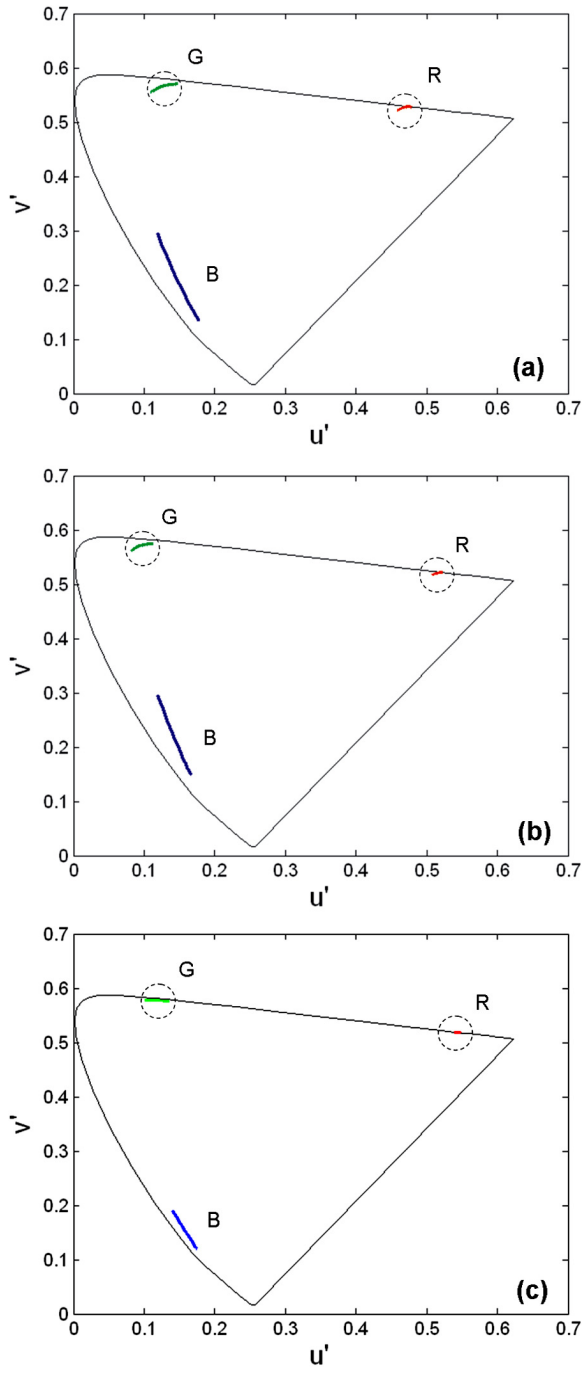

FIGURE 4 — The plot of the CIE 1976 UCS diagrams with different incident angles at the gray level, G63, for different backlights. (a) CCFL, (b) white LED, and (c) RGB-LED.

TABLE 1 — The calculated $\Delta u'v'$ values of the film-compensated MVA-LCDs at different gray levels with three different backlights. θ varied from –80° to 80°, and every θ is scanned across the whole 360° azimuthal angle (ϕ) at 10° scanning step.

MVA		CCFL + CF	LED + CF	RGB – LED
G63	R	0.0206	0.0146	0.0097
	G	0.0423	0.0343	0.0322
	B	0.1724	0.1545	0.0729
G255	R	0.0164	0.0115	0.0089
	G	0.0385	0.0319	0.0295
	B	0.1495	0.1394	0.0594

To quantitatively characterize the angular color uniformity under different backlights and different gray levels, we redefine Eq. (3) as

$$\Delta u'v' = \sqrt{(u'_{\max} - u'_{\min})^2 + (v'_{\max} - v'_{\min})^2}, \qquad (12)$$

where $[u'_{\max}, v'_{\max}]$ and $[u'_{\min}, v'_{\min}]$ represent the maximum and minimum $[u', v']$ values at the low gray level, G63, and the full bright state, G255. The detailed results are shown in Table 1.

For the angular color shift of the film-compensated MVA-LCD for a CCFL BLU plus color filters at G63, we obtain $\Delta u'v'$ = (0.0206, 0.0423, 0.1724) at the RGB primaries. When an LED BLU is used, we obtain $\Delta u'v'$ = (0.0097, 0.0322, 0.0729) when using a white LED BLU with color filters and $\Delta u'v'$ = (0.0089, 0.0295, 0.0594) for an RGB LED BLU without color filters at the respective RGB primaries. The white-LED-lit MVA-LCD shows a 1.1–1.4× better angular color uniformity in the RGB primaries than the CCFL-based MVA-LCD. Noticeably, the RGB-LED backlit MVA-LCD has much evident improvement, which shows ~1.3× better angular color uniformity in green and ~2.0× in red and blue primaries than the CCFL-based MVA-LCD.

As for the angular color shift of a film-compensated MVA-LCD under a different backlight at gray level, G255, a similar angular color-uniformity improvement trend can be seen as at the low gray level, G63. The white-LED-backlit MVA-LCD shows a limited 1.1–1.4× angular color uniformity in RGB primaries than the CCFL-based MVA-LCD, while when the RGB-LED backlight is used, the improvement is more evident, *e.g.*, the angular color uniformity in green is improved by ~1.30×, ~2× in red, and ~2× in blue primaries than the CCFL-based MVA-LCD. In short, the LED-backlit MVA-LCDs show better angular color uniformity than the CCFL-based MVA-LCD at the different gray levels.

4.3 Color shift in the horizontal direction

In evaluating the color uniformity of an LCD monitor or TV, the observers care more about the color performance in the horizontal and vertical directions. Therefore, the color shift in the horizontal direction is usually measured. Figure 5 shows the simulated angular dependent $\Delta u'v'$ of an MVA-LCD backlit by different light sources as observed from the horizontal (ϕ = 0°) viewing direction at G63 and G255, respectively. The RGB curves are more or less symmetric along θ = 0° and the $\Delta u'v'$ value increases as θ increases. It is interesting to note that no matter which backlight is used, blue color always has the largest $\Delta u'v'$ value, followed by green and then red. During the simulation, we set an optimized LC phase retardation to maximize the light efficiency of the MVA-LCD for the green primary at normal incident angle. Based on the birefringence dispersion of the LC material as defined in Eq. (4), we can see that the light transmittance in Eq. (11) is more easily influenced by the shorter wavelength (blue color) than the longer wavelength (red color). This explains why the MVA-LCD always exhibits the largest $\Delta u'v'$ values in blue color while the smallest one in red color.

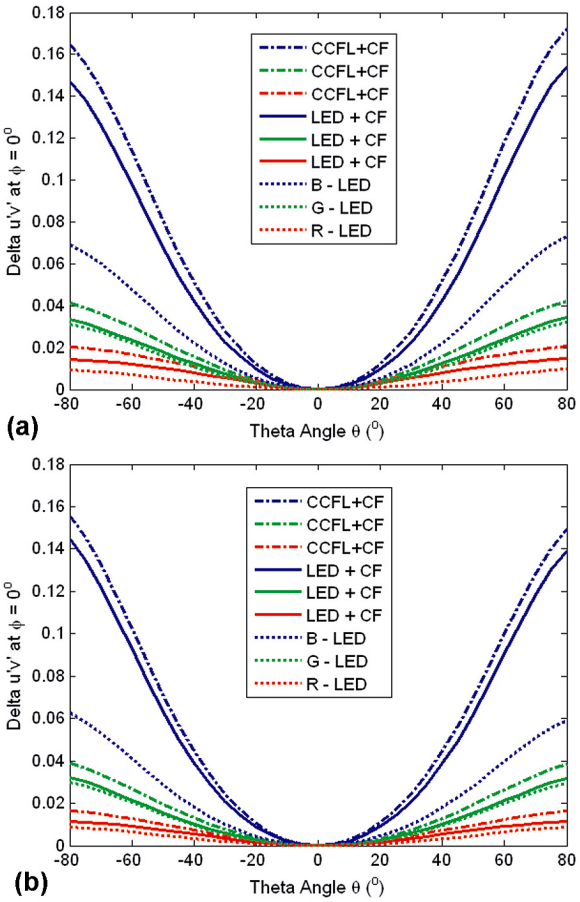

FIGURE 5 — Color shift for RGB primaries at the different gray levels under different backlights along the horizontal direction. (a) Gray level, G63; (b) gray level, G255.

In the region where |θ| > 0, the $\Delta u'v'$ of white-LED-backlit MVA-LCD with CFs is smaller than that of the CCFL BLU with CFs for the respective RGB primaries. At G63 low gray level, as shown in Fig. 5(a), $\Delta u'v'$ = (0.0146, 0.0341, 0.1544) for a white LED and $\Delta u'v'$ = (0.0206, 0.0421, 0.1724) for a CCFL at the respective RGB primaries at θ = 80°. Figure 5(b) shows the calculated $\Delta u'v'$ = (0.0115, 0.0319, 0.1394) at G255 for a white LED and $\Delta u'v'$ = (0.0164, 0.0384, 0.1495) for a CCFL at

the respective RGB primaries at θ = 80°. In addition, it is noticeable that with the increase of gray levels, the corresponding angular-dependent color shift is reduced. This is because the LC molecules are bent more effectively at higher gray levels which, in turn, lessen the angular-dependent effect of LC phase retardations at the off-axis angles as the case of in-plane-switching (IPS) LCDs.[19] From Fig. 5, it indicates that an LED backlight is helpful in reducing color shift.

Also found in Fig. 5, for each RGB primary the color shift of an RGB LED is much smaller than that of LEDs and CCFLs with color filters. At θ = 80°, the $\Delta u'v'$ values for the RGB primaries of the RGB-LED system are as low as (0.0097, 0.0322, 0.0729) for G63 and (0.0089, 0.0296, 0.0593) for G255, which is ~1.3–2.5× smaller than a conventional CCFL-BLU system. This weaker color shift results from a narrower spectral bandwidth and less overlap of the RGB LED light sources, which limits the wavelength-dependent light transmittance, T, in a narrow spectral range for the integration of S(λ) in Eq. (1) as discussed in Sec. 4.2.

4.4 Gamma curves at different viewing angles

Luminance is usually used as the quantitative brightness measure of an LCD. Since the human eye's sensitivity to light is not linear, the gamma correction for the different gray levels in a LCD should be considered, which is based on the voltage-dependent transmittance curve of the LCD cell.[20] Figure 6(a) plots the gamma curves of the MVA-LCD at different oblique viewing angles under white-LED and CCFL backlights. Here, a light skin color of [R, G, B] = [241, 149, 108] is used; the azimuthal angle is set at 0°, the polar angle θ varies from 0° to 60°, and the gamma factor γ = 2.2. The MVA-LCD has a fairly large gamma variation when the off-axis oblique viewing angle is larger than 40°, especially in the low and middle gray levels, no matter what type of backlight is used. It indicates that a MVA-LCD has color washout when observed from oblique angles.

As can be seen from Eq. (9), the angular-dependent phase retardation of the LC medium at a given wavelength λ is determined by the applied voltage on the MVA-LCD. Consequently, the light transmittance (T) through the LC medium under crossed linear polarizers is also closely related to the applied voltage at different gray levels. In the voltage-off state of the simulated MVA-LCD, the LC directors are vertically aligned on the substrate surfaces. When the applied voltage exceeds a threshold, the LC directors are tilted out of plane by the longitudinal electric field. In the low-to-medium gray levels, the LC molecules are partly bent away from the substrate normal. The tilt angle has a sinusoidal distribution across the LC layer. As disclosed in Eqs. (9)–(11), the voltage-dependent transmittance curve would be largely influenced by the LC tilt angle and the non-zero polar angle θ at an oblique viewing direction, regardless of which type of backlit is employed. Therefore, at low and medium gray levels, the MVA-LCD has a certain degree of gamma variation at an off-axis viewing angle, and this trend is less influenced by the backlight adopted.

For comparison, the gamma curves of an IPS-LCD at different oblique viewing angles under the same white-LED and CCFL backlights are also plotted in Fig. 6(b). The device configuration is shown in Ref. 21. From Fig. 6(b), the gamma curves of the IPS-LCD are less influenced by the variation of the backlights. By contrast, the IPS-LCD has less color washout than the MVA-LCD at oblique off-axis viewing angles. This is because the applied transverse electric fields mainly rotate the LC directors in the same plane while the out-of-plane tilt component is minimal in an IPS-LCD. However, its contrast ratio at a normal viewing direction is lower than that of MVA-LCDs.[22,23] An effective method to improve the off-axis gamma curves of an MVA-LCD is to employ the dual-threshold approach in which a unit pixel is divided into two subpixels and each subpixel exhibits a different threshold voltage.[24]

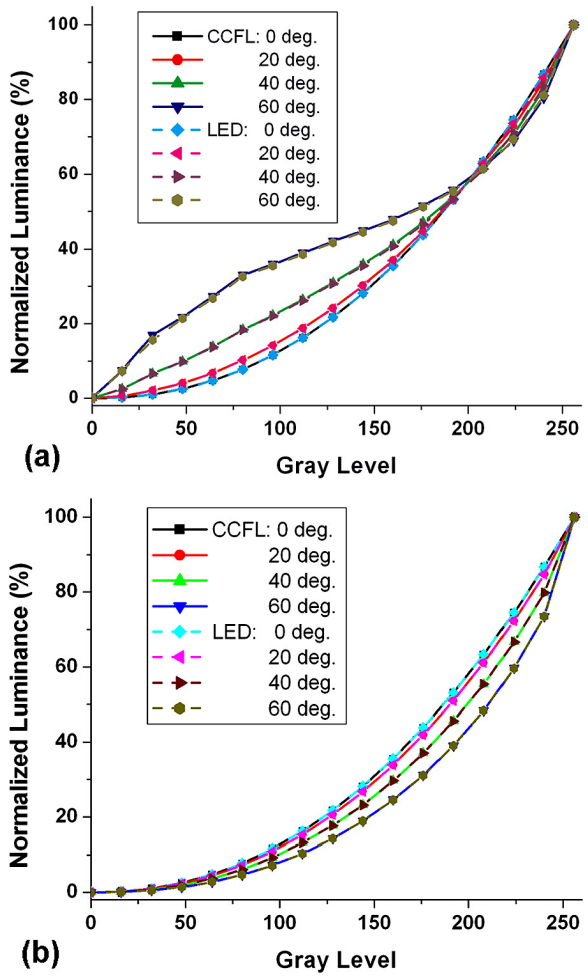

FIGURE 6 — The gamma curves of (a) the MVA and (b) IPS LCD at light skin color under white-LED and CCFL backlights.

5 Conclusions

The color performance of an MVA-LCD is quantitatively evaluated in terms of color gamut, color shift, and gamma curves using white LEDs, RGB-LEDs, and CCFLs as backlights. The LED-backlit LCDs not only exhibit a wider color gamut but also has an ~1.3–2.5× smaller color shift than that of a CCFL-BLU, especially when no color filters are used. In the meantime, the angular-dependent gamma curves are less influenced by the variation of the backlights. The obtained quantitative results are useful for optimizing the color performances, and color management of high-end LCD monitors and LCD TVs.

Acknowledgments

The authors are indebted to the financial support of Chi-Mei Optoelectronics Corporation (Taiwan).

References

1 G. Harbers and C. Hoelen, *SID Symposium Digest* **32**, 702 (2001).
2 G. Harbers, W. Timmers, and W Sillevis-Smitt, *J. Soc. Info. Display* **10**, 347 (2002).
3 H. S. Hsieh, C. H. Chou, and W. Y. Li, *Proc. Intl. Display Manufacturing Conf.*, 622–624 (2005).
4 R. Lu, X. Zhu, S. T. Wu, Q. Hong, and T. X. Wu, *J. Display Technol.* **1**, 3 (2005).
5 J. J. Lyu, J. Sohn, H. Y. Kim, and S. H. Lee, *J. Display Technol.* **3**, 404 (2007).
6 G. Wyszecki and W. Stiles, *Color Science – Concepts and Methods, Quantitative Data and Formulate*, 2nd edn. (Wiley, New York, 1982).
7 R. Hunt, *Measuring Colour*, 2nd edn. (Ellis Horwood, West Sussex, 1991).
8 S. Kim, *SID Symposium Digest* **35**, 760 (2004).
9 S. T. Wu, *Phys. Rev. A* **33**, 1270 (1986).
10 J. Li and S. T. Wu, *J. Appl. Phys.* **95**, 896 (2004).
11 S. T. Wu and D. K. Yang, *Reflective Liquid Crystal Displays* (Wiley, New York, 2001).
12 Q. Hong, T. X. Wu, X. Zhu, R. Lu, and S. T. Wu, *Appl. Phys. Lett.* **86**, 121107 (2005).
13 S. T. Wu, *Mater. Chem. Phys.* **42**, 163 (1995).
14 A. Lien, *Liq. Cryst.* **22**, 171 (1997).
15 Z. Ge, X. Zhu, T. X. Wu, and S. T. Wu, *J. Opt. Soc. Am. A* **22**, 966 (2005).
16 M. F. Hsieh, K. H. Peng, Y. H. Hsu, M. C. Shih, H. C. Hung, C. P. Hung, H. S. Hsieh, W. Y. Li, M. T. Yang, and C. K. Wei, *SID Symposium Digest* **37**, 1942 (2006).
17 S. T. Wu, "Phase-matched biaxial compensation film for LCDs," *SID Symposium Digest* **26**, 555 (1995).
18 S. T. Wu, U. Efron, and L. D. Hess, *Appl. Opt.* **23**, 3911 (1984).
19 C. H. Oh, H. M. Moon, W. K. Yoon, J. H. Kim, M. H. Song, J. J. Kim, J. H. Lee, J. H. Kim, C. S. Im, S. W. Lee, H. C. Choi, and S. D. Yeo, *J. Soc. Info. Display* **12**, 11 (2004).
20 W. den Boer, *Active Matrix Liquid Crystal Displays: Fundamentals and Applications* (Elsevier Inc., 2005).
21 R. Lu, Q. Hong, Z. Ge, and S. T. Wu, *Opt. Express* **14**, 6243 (2006).
22 H. C. Jin, I. B. Kang, E. S. Jang, H. M. Moon, C. H. Oh, S. H. Lee, and S. D. Yeo, *J. Soc. Info. Display* **15**, 277 (2007).
23 H. K. Hong, H. H. Shin, and I. J. Chung, *J. Display Technol.* **3**, 361 (2007).
24 R. Lu, S. T. Wu, and S. H. Lee, *Appl. Phys. Lett*. **92**, 051114 (2008).

Ruibo Lu received his Ph.D. from the Department of Physics, Fudan University, China, in 1998, and his M.S. degree in applied physics from East China University of Science and Technology, China, in 1995. He is a research scientist at the College of Optics and Photonics, University of Central Florida. His research interests include liquid-crystal-display technology, liquid-crystal components for optical communications, and optical imaging using liquid-crystal medium. He is a member of SID.

Xiangyi Nie received his B.S. and M.S. degrees in electrical engineering from Nanjing University, Nanjing, China, in 1999 and 2002, respectively, and his Ph.D. degree in electrical engineering from the University of Central Florida in 2007. He joined Sony Ericsson Mobile Communications (U.S.A.) Inc. in 2007 as a display engineer.

Shin-Tson Wu received his Ph.D. from the University of Southern California and his B.S. degree in physics from National Taiwan University. He is a PREP Professor at the College of Optics and Photonics, University of Central Florida. His studies at UCF concentrate in foveated imaging, bio-photonics, optical communications, liquid-crystal displays, and liquid-crystal materials. He is a Fellow of the IEEE, SID, and OSA.